**Les Cahiers du GERAD** ISSN: 0711–2440

# Mean Field Game-based control of sharing daily solar energy between electric vehicles in a parking lot

S. M. Muhindo, R. P. Malhamé, G. Joós

G–2021–29

May 2021



La publication de ces rapports de recherche est rendue possible grâce au soutien de HEC Montréal, Polytechnique Montréal, Université McGill, Université du Québec à Montréal, ainsi que du Fonds de recherche du Québec – Nature et technologies.

Dépôt légal – Bibliothèque et Archives nationales du Québec, 2021
– Bibliothèque et Archives Canada, 2021

The publication of these research reports is made possible thanks to the support of HEC Montréal, Polytechnique Montréal, McGill University, Université du Québec à Montréal, as well as the Fonds de recherche du Québec – Nature et technologies.

Legal deposit – Bibliothèque et Archives nationales du Québec, 2021
– Library and Archives Canada, 2021

**GERAD** HEC Montréal
3000, chemin de la Côte-Sainte-Catherine
Montréal (Québec) Canada H3T 2A7

**Tél. : 514 340-6053**
Téléc. : 514 340-5665
info@gerad.ca
www.gerad.ca

# Mean Field Game-based control of sharing daily solar energy between electric vehicles in a parking lot

**Samuel M. Muhindo** [a, b, c]

**Roland P. Malhamé** [a, b, c]

**Géza Joós** [d, c]

[a] *GERAD, Montréal (Québec) Canada, H3T 2A7*

[b] *Department of Electrical Engineering, Polytechnique Montréal, Montréal (Québec) Canada H3T 1J4*

[c] *Réseau québécois sur l'énergie intelligente (RQEI), Trois-Rivières (Québec) Canada, G9A5H7*

[d] *Department of Electrical and Computer Engineering, McGill University, Polytechnique Montréal, Montréal (Québec) Canada, H3A 0E9*

samuel.muhindo-mugisho@polymtl.ca
roland.malhame@gerad.ca
geza.joos@mcgill.ca

**May 2021**
**Les Cahiers du GERAD**
**G–2021–29**

**Abstract :** This paper develops a strategy, using concepts from Mean Field Games, to coordinate the charging of a large population of battery electric vehicles (BEVs) in a parking lot powered by solar energy and managed by an aggregator. The goal is to share the energy available so as to minimize the standard deviation of the state of charge (SoC) of batteries at the end of the day. We consider both cases of homogeneous and heterogeneous populations of BEVs with a stochastic dynamics of SoC. The charging laws correspond to the Nash equilibrium induced by quadratic cost functions based on an inverse Nash equilibrium concept and designed to help the batteries with the lowest initial SoCs. While the charging laws are strictly decentralized, they guarantee that a *weighted* mean of instantaneous charging powers to the vehicles follows a mean charging trajectory based on the solar energy forecast for the day. That day ahead forecast is broadcasted to the vehicles which can then gauge the necessary SoC upon leaving their home. We illustrate the advantages of our strategy in the two cases of a typical sunny day and a typical cloudy day when compared to more straightforward strategies: *first come first full* and *equal sharing*.

**Keywords:** Aggregator, battery electric vehicle, Mean Field Games, Nash equilibrium, parking lot, solar energy

**Acknowledgements:** The authors would like to sincerely thank Kato Vanroy from the department of Mechanical Engineering at Polytechnique Montreal for practical utilization of the TRNSYS software and Quentin Lénet for the first steps in inverse Nash algorithm. This work was supported by the *Réseau Québécois sur l'énergie Intelligente* (RQEI).

# 1 Introduction

The massive introduction of BEVs in modern power systems is bound to have important impacts, positive or negative, depending on the way this novel situation is managed [16]. There will be a great pressure to introduce numerous charging stations where the need is anticipated, but if too many high speed charging vehicles are connected at any one time (for example upon departure from work towards residence place), that may create both local transformer and eventually system wide overloads [13]. On the other hand, adequate management of the battery storage associated with an aggregate of BEVs can turn such an aggregate into a virtual power plant. Thus, in a context of integration with clean sources of energy, such as photovoltaics, car batteries could be storing the solar energy available during the day when cars are parked [3, 5, 7]. As is well known in the photovoltaics rich state of California for example, a so-called power demand *duck curve* [4] is observed: the peak demand occurs at the end of the day, upon return of working people to their homes. At that point, available solar radiation has all but disappeared and while solar energy may have been used by consumers during the day, there is a need for a high electric power ramp at dusk followed by several hours of sustained high power consumption. The latter power demand will be most likely met by fossil based energy sources, unless some other mitigating actions are taken. In [6, 14], the authors show in their context, that if the electric energy storage contained in a large number of BEVs is properly utilized, this could help significantly reduce the power needed from fossil sources during the evening peak.

Our objective in this paper is to propose an algorithm with desirable properties, for sharing solar photovoltaic (PV) power amongst BEVs parked in a parking lot, or a collection of federated parking lots. The cars belong to commuters working in the neighborhoods of these parking lots and could recharge at least partially depending on sunshine availability, their batteries at the parking lot charging stations. One particular business model is that the parking lots aggregator would charge a yearly fee for use of a parking space and the associated charging station. If then the car owners wish to recuperate part of their parking costs or even make an extra amount of profit, they could choose to participate in a financially compensated grid support operation coordinated by the aggregator.

In prior recent work, the authors in [10] proposed a *linear programming* (LP) strategy, in a solar powered parking lot of a car-share service to fairly distribute the available solar energy amongst heterogeneous BEVs by favoring those arriving with less charge. They studied the case where the supply demand ratio (SDR) is strictly inferior to 1. They demonstrated, by charging a subset of BEVs during each time slot, a reduction of 60% of yearly average standard deviation in the battery charge levels at the end of recharging compared to the *equal sharing* (ES) approach. In [19], the authors studied the case when it is not possible to charge all BEVs simultaneously at their homes. They developed a centralized *weighted fair queuing* (WFQ) algorithm with a time slot control switch in each smart charger to charge maximally all of the homogeneous BEVs, by favoring (i.e. charging more quickly) those arriving with less charge. The strategy selected then a subset of BEVs to charge in each interval during peak demand when there is not enough energy. They compared the results with a *first come first full* (FCFF) algorithm. They showed that when the SDR is equal to 1, there is 5% of BEVs which cannot leave their homes on time while it is 7% for FCFF.

In both works above which come close to what we are going to do, the authors failed to propose a *decentralized* algorithm. A decentralized control scheme allows individual BEVs to determine their own charging pattern. Their decisions could, for example, be made on the basis of time-of-day, electricity price or battery state of health [12, 18]. We suggest relying on an adequately tailored variation of a Mean Field Game-based control scheme [8, 9] which, while it fills all cars simultaneously, tends to provide more instantaneous charging to the cars with the lowest current fill levels. The problem can be formulated as large population game on a finite charging interval. In [12], the authors study the existence, uniqueness and optimality of the Nash equilibrium of the charging problems to minimize local electricity costs and to fully charge. In a decentralized computational mechanism, they show in a deterministic case that the large population charging games will converge to a unique Nash equilibrium which is either globally optimal for a homogeneous population or nearly globally optimal for heterogeneous population.

Most of the rest of literature [6, 12, 15, 17, 18] is directly based on *economic incentives* and thus does not concern us in this paper. The authors address BEVs charging strategies where the charging is scheduled according to the energy price and/or the distribution system losses to the grid.

The table below places our work in the BEVs charging optimization when the aggregators are parking lot operators (PLOs) and distribution grid operators (DGOs).

**Table 1: Classification of related work in the literature.**

| | *Potential goal* | | |
|---|---|---|---|
| **Aggregators** | user satisfaction | monetary benefits | grid impact |
| PLOs | our work, [10] | [6, 12] | [15] |
| DGOs | [19] | [18] | [17] |

The charging control strategies tested in this paper will be compared with respect to the following requirements:

- *fairness*: we wish that for each user, at the end of recharging in the parking lot, the SOC of its BEV will end up close to the average of that of all other users, regardless of the BEV's initial SOC. Thus, we look for a charging scheme to favour the emptier SOCs when compared to the fuller ones upon arrival in the parking lot. However, at no time, the SOCs which were initially lower should be permitted to exceed the ones that were initially higher. Note that in *Appendix C*, we define a fairness coefficient and use it to contrast the performance of various charging strategies.
- *decentralization* and *non-invasiveness*: from the point of view of the parking lot operator, decentralized charging control laws are quite desirable because they minimize the need to observe the state of charge of individual batteries, a process which is both complex and invasive. Furthermore, a local control allows a user to interrupt the process at any time, particularly if the parking operator has designed a charging scheme based on a poor model of the battery.

In what follows we shall present the Mean Field Game-based algorithm to calculate the proposed operator dictated decentralized control laws according to the potential solar energy available. Subsequently, the performance of these laws will be compared to that of two common strategies used in the literature. The first strategy (*first come first full*) [19] consists in maximally recharging the BEVs in order of arrival at the parking lot. The second strategy (*equal sharing*) [10] consists in sharing equally at all times the available solar power amongst battery vehicles still not fully charged. All strategies make full use of the available daily energy. Also, for the purpose of meaningfully comparing the performance of the different strategies in our case studies, we assume that the SDR is less than one.

## Limitations of proposed control algorithm

In order to implement our charging strategy, we make the following assumptions:

- We assume an existence of an infrastructure to *coordinate* BEVs charging in the parking lot and PV production with a SDR *strictly inferior to 1*.
- We assume a *fixed* number of BEVs which are charged in the parking lot *simultaneously*.
- The BEVs are charged according to a *local state feedback law*, determined by the parking lot operator, with common structure for all BEVs within the same category. Thus, the charging rate is *controlled* in the charger.

The rest of this paper is organized as follows. In Section 2, we present the theoretical underpinnings and details of our proposed algorithm. In Section 3, we present the results in the homogeneous case. In Section 4, we present the results in the heterogeneous case. Finally, in Section 5, we conclude and give an outlook on future research.

# 2 Mean Field Game-based control of a large population of homogeneous BEVs

## 2.1 Nomenclature

| | |
|---|---|
| $\mathbb{E}$ | mathematical expectation symbol |
| $\nabla$ | vector differential operator |
| $\partial\square/\partial\triangle$ | partial derivative of $\square$ with respect to $\triangle$ |
| $d\triangle$ | differential of $\triangle$ |
| $t, T$ | time *and* time at steady state (i.e. $t \to \infty$) |
| $i$ | a user of BEV |
| $c$ | homogeneous class of BEVs |
| $\triangle_{i,t,c}$ | any parameter $\triangle$ below applied in $\{i, t, c\}$ |
| $\alpha$ | charging efficiency of the battery |
| $\beta$ | capacity of the battery |
| $b = \alpha/\beta$ | characteristic of the battery |
| $J, J^*$ | cost to minimize *and* optimal cost |
| $u, u^*$ | charging power *and* optimal charging power |
| $u_W$ | daily solar power curve in the parking |
| $W$ | total daily solar energy in the parking |
| $W_c$ | class weighted daily solar energy in the parking |
| $x$ | state of charge (SoC) of BEV |
| $x_{i,0\|\infty}$ | initial/final SoC of BEV's user $i$ |
| $\overline{x}_{0\|\infty}$ | average initial/final SoCs of BEVs |
| $\overline{x}_t$ | mathematical expectation of SoC of BEVs |
| $\overline{x}_t^{target}$ | target for mean SoC of BEVs |
| $\overline{x}_\infty^{target}$ | target for steady-state mean SoC of BEVs |
| $\sigma_{x_{i,0\|\infty}}$ | standard deviation of initial/final SoCs |
| $q_t^y$ | pressure field trajectory for all BEVs |
| $q_\infty^y$ | steady state pressure field for all BEVs |
| $q_{x_0}$ | comfort coefficient of all BEVs |
| $r$ | control coefficient of all BEVs |
| $y$ | collective direction of BEVs' SoCs |
| $\delta$ | discount factor for convergence of the cost $J$ |
| $\nu, \omega$ | Brownian noise intensity *and* Brownian motion |
| $\pi$, $s$, $\gamma$ | coefficients of quadratic form of optimal cost $J^*$ |

## 2.2 Mathematical model

We consider a large population of $N$ homogeneous BEVs in a parking lot. The assumption of a *large* population is needed because later on in our analysis, we will assimilate the empirical mean of SoCs (a random quantity for a *small* number of vehicles) with its mathematical expectation (a predictable deterministic quantity) by virtue of *the law of large numbers*. Each BEV $i$, $i = 1, ..., N$, has an initial SoC $x_{i,0}$ which results of a daily traffic pattern from home to parking. We can then write the SoC stochastic dynamics for BEV $i$ as follows:

$$dx_{i,t} = bu_{i,t}dt + \nu d\omega_i,\ t \geq 0, \tag{1}$$

where $t \in [0, T]$ is in $h$, $x_{i,t}$ is the SoC in $\mathtt{pu}$, $b = \frac{\alpha}{\beta}$, $\alpha \in (0, 1]$ is the charge efficiency of the battery in $\mathtt{pu}/h$, $\beta$ is the battery capacity in $kWh$, $u_{i,t} \in \mathbb{R}^+$ is the charging power in $kW$, $\omega_i$ is a normalized Brownian process, $\nu$ is the intensity of that Brownian noise and $\omega_i$ is assumed independent of $\omega_j$ for $i \neq j$. The term $\nu d\omega_i$ defines the *stochasticity* of the SoC which can result physically from fluctuations in the charging and losses of the battery.

## 2.3 Considerations

We wish to address the decentralized control of battery recharging of a set of BEVs as part of a so-called Mean Field Game (MFG). One can refer to *Appendix A* for a short description of the basic concepts in MFG. The control will be of linear-quadratic (LQ) type [9]. The parking lot operator broadcasts an average SoC target trajectory ($\overline{x}_t^{target}$) based on the solar energy forecast for the current day. The goal is that the BEVs store up as much of the solar energy available as possible and stabilize when sunshine subsides at a precalculated steady-state average SoC ($\overline{x}_\infty^{target}$) based on the forecast. The proposed algorithm requires that the parking lot operator know the average SoC of the BEVs upon arrival ($\overline{x}_0$). This can be achieved by recording initial SoCs as BEVs enter the parking lot.

The focal point of the approach is the prescription of a daily quadratic cost $J_i$ for each BEV $i$ to ensure that the BEVs that are initially fuller recharge less quickly than those that are less full, so that final SoC standard deviation is reduced; while still maintaining the collective goal of bringing all BEVs to a steady-state average target SoC. The cost functions are designed so that by optimizing the individual BEV costs $J_i$, one achieves the aggregator's goal. The latter is that the average SoC trajectory ($\overline{x}_t$) exactly match the average SoC target trajectory ($\overline{x}_t^{target}$) and computed based on the sunshine forecast.

## 2.4 Establishment of individual battery cost function

The battery cost function on an infinite horizon is a mathematical expectation. It is designed by the aggregator and defined for a BEV as follows:

$$\begin{aligned} J_i(x_{i,0}, u_{i,t}) =& \mathbb{E}\Big[ \int_0^\infty e^{-\delta t} \big[ \frac{q_t^y}{2}(x_{i,t} - y)^2 + \frac{r}{2} u_{i,t}^2 \\ &+ \frac{q_{x_0}}{2}(x_{i,t} - x_{i,0})^2 \big] dt \mid x_{i,0} \Big], \end{aligned} \tag{2}$$

where $\delta$ is a discount coefficient to ensure convergence of the cost (we could set $\delta$ to zero to work on a finite horizon $T$), $y$ is the collective direction of the BEVs' SoCs which is equal to 1 in our case (it serves as a direction signal to all BEVs, such that all BEVs should move toward $y$ but not beyond), $r$ is a coefficient which penalizes the level for charging rate, $q_{x_0}$ is a pressure coefficient aimed at limiting the distance from the initial SoC (for the state of health of the user's battery and fairness to others) and $q_t^y$ is the pressure field trajectory. The latter is common to all BEVs and is numerically obtained as the solution of a *system of differential equations*. It is the key quantity which will drive all SoCs towards a full state of charge while sharing instantaneously available solar energy in a way that reduces the variance of SoCs. Its computation is more detailed below and it is at the heart of our inverse Nash equilibrium procedure. The class of quadratic cost functions is well documented in the literature [8, 9, 11].

The BEVs will collectively recharge their batteries with a time dependent coefficient ($q_t^y$) penalizing the gap between the current SoC ($x_{i,t}$) and the ultimate destination direction of SoCs defined by the value of $y$. Once the target ($\overline{x}_\infty^{target}$) is reached, $q_t^y$ will settle to a constant value, allowing the reaching of an SoC steady state that meets the constraints set by the parking lot operator.

## 2.5 Optimal control problem and solutions

We begin by making the following variable changes to simplify the expression of cost $J_i$ in Equation (2):

$$\begin{aligned} X_{i,t} = (x_{i,t} - y)e^{-\delta t/2}, U_{i,t} = u_{i,t}e^{-\delta t/2}, \\ V_t = \nu e^{-\delta t/2} \text{ and } Z_{i,t} = (x_{i,t} - x_{i,0})e^{-\delta t/2}. \end{aligned} \tag{3}$$

Then

$$\begin{aligned} dX_{i,t} &= dx_{i,t}e^{-\delta t/2} - \frac{\delta}{2}x_{i,t}e^{-\delta t/2}dt + \frac{\delta}{2}ye^{-\delta t/2}dt \\ &= (bu_{i,t}dt + \nu d\omega_i)e^{-\delta t/2} - \frac{\delta}{2}(x_{i,t} - y)e^{-\delta t/2}dt \\ &= -\frac{\delta}{2}X_{i,t}dt + bU_{i,t}dt + V_t d\omega_i. \end{aligned} \tag{4}$$

The principle of resolution is based on assuming a quadratic form of the optimal cost function (with coefficients $\pi, s$ and $\gamma$):

$$J_i^*(X_{i,t}) = \frac{1}{2}\pi_{i,t}X_{i,t}^2 + s_{i,t}X_{i,t}e^{-\delta t/2} + \gamma_{i,t}. \tag{5}$$

We then write the Hamilton-Jacobi-Bellman equation corresponding to this assertion [1].

$$\frac{\partial J_i^*}{\partial t} + \min_U \Big\{ \frac{q_t^y}{2}X_{i,t}^2 + \frac{q_{x_0}}{2}Z_{i,t}^2 + \frac{r}{2}U_{i,t}^2 + \frac{\partial J_i^*}{\partial X}\big(-\frac{\delta}{2}X_{i,t} + bU_{i,t}\big) + \frac{\partial^2 J_i^*}{\partial X^2}\frac{V_t^2}{2}\Big\} = 0. \tag{6}$$

Differentiating with respect to $U_{i,t}$ yields

$$\begin{aligned} &\nabla_U\big\{\frac{q_t^y}{2}X_{i,t}^2 + \frac{q_{x_0}}{2}Z_{i,t}^2 + \frac{r}{2}U_{i,t}^2\big\} + \nabla_U\Big\{\frac{\partial J_i^*}{\partial X}\big(-\frac{\delta}{2}X_{i,t} + bU_{i,t}\big) + \frac{\partial^2 J_i^*}{\partial X^2}\frac{V_t^2}{2}\Big\} = 0 \\ &\longrightarrow U_{i,t}^* = -\frac{b}{r}\frac{\partial J_i^*}{\partial X}. \end{aligned} \tag{7}$$

The second derivative with respect to $U_{i,t}$ is $r > 0$, so the value found will indeed correspond to a minimum:

$$U_{i,t}^* = -\frac{b}{r}\big[\pi_{i,t}X_{i,t} + s_{i,t}e^{-\delta t/2}\big]. \tag{8}$$

The optimal control therefore depends on the values $\pi_{i,t}$ and $s_{i,t}$. The expressions of $\pi_{i,t}$ and $s_{i,t}$ are then determined by identification:

$$\begin{aligned} \frac{1}{2}X_{i,t}^2\frac{d\pi_{i,t}}{dt} + X_{i,t}e^{-\delta t/2}\big(\frac{ds_{i,t}}{dt} - \frac{\delta}{2}s_{i,t}\big) + \frac{d\gamma_{i,t}}{dt} =& -\frac{q_t^y}{2}X_{i,t}^2 - \frac{q_{x_0}}{2}Z_{i,t}^2 + \frac{b^2}{2r}\big(\pi_{i,t}^2X_{i,t}^2 + 2X_{i,t}\pi_{i,t}s_{i,t}e^{-\delta t/2} \\ &+ s_{i,t}^2e^{-\delta t}\big) + \frac{\delta}{2}X_{i,t}\big(\pi_{i,t}X_{i,t} + s_{i,t}e^{-\delta t/2}\big) - \frac{V_t^2}{2}\pi_{i,t} \\ =& X_{i,t}^2\big(\frac{b^2}{2r}\pi_{i,t}^2 + \frac{\delta}{2}\pi_{i,t} - \frac{q_t^y}{2} - \frac{q_{x_0}}{2}\big) \\ &+ X_{i,t}e^{-\delta t/2}\big(\frac{b^2}{r}\pi_{i,t}s_{i,t} + \frac{\delta}{2}s_{i,t} - yq_{x_0} + x_{i,0}q_{x_0}\big) + \dots. \end{aligned} \tag{9}$$

The resulting coupled differential equations are:

$$\begin{aligned} \frac{d\pi_{i,t}}{dt} &= \frac{b^2}{r}\pi_{i,t}^2 + \delta\pi_{i,t} - q_t^y - q_{x_0}, \\ \frac{ds_{i,t}}{dt} &= (\delta + \frac{b^2}{r}\pi_{i,t})s_{i,t} + q_{x_0}(x_{i,0} - y). \end{aligned} \tag{10}$$

This leads to the optimal control law:

$$u_{i,t}^* = -\frac{b}{r}\big[\pi_{i,t}(x_{i,t} - y) + s_{i,t}\big]. \tag{11}$$

The coefficient $q_t^y$ appearing in the differential equation of $\pi$ is unknown at this stage. Nonetheless, it must respect the fact that when the BEVs use the optimal control $u_{i,t}^*$, their empirical average

trajectory ($\overline{x}_t$), *assimilated thanks to the law of large numbers to the mathematical expectation of the SoC of a generic BEV* ($\mathbb{E}[x_{i,t}]$), will correspond to the average target trajectory ($\overline{x}_t^{target}$) imposed by the parking lot operator. The control strategy that is developed, relies on knowing the anticipated solar energy during the day. Based on the dynamics of the SoC $x_{i,t}$ in Equation (1), the average target $\overline{x}_t^{target}$ needed is determined by integrating the curve of anticipated total solar power ($u_{W_t}$) over the time horizon $T$ of interest and dividing, for a case of homogeneous battery capacities, by the total number of BEVs present in the parking lot for recharging. The total daily solar energy available ($W = \int_0^T u_{W_t} dt$) is assumed less than the total energy that all BEVs would need to fully recharge their batteries.

## 2.6 Calculation of $q_t^y$ by Nash equilibrium inversion

We calculate the pressure field $q_t^y$ directly by numerical resolution of differential equations. This system of differential equations to be solved is obtained by imposing that under the action of $q_t^y$, and the associated optimal control law (Equation (11)), the average trajectory $\overline{x}_t$ of the BEVs follow the average target trajectory $\overline{x}_t^{target}$ dictated by the parking lot operator. This restriction allows us to write the Mean Field equations based on taking the mathematical expectation of the SoC of a generic battery in the population subject to decentralized control law (Equation (11)).

$$\begin{aligned}
\frac{d\overline{x}_t^{target}}{dt} &= b\overline{u}_t^* = -\frac{b^2}{r}[\pi_t(\overline{x}_t^{target} - y) + \overline{s}_t], \\
\frac{d\pi_t}{dt} &= \frac{b^2}{r}\pi_t^2 + \delta\pi_t - q_t^y - q_{x_0}, \\
\frac{d\overline{s}_t}{dt} &= (\delta + \frac{b^2}{r}\pi_t)\overline{s}_t + q_{x_0}(\overline{x}_0 - y).
\end{aligned} \tag{12}$$

With this approach, the goal is to obtain a mathematical relationship between $\frac{d\overline{x}_t^{target}}{dt}$ and $q_t^y$. This is the so-called *inverse Nash algorithm*, its first steps were developed in the control of electric space heaters [11].

With the first Equation of (12), we can write the relation between $\pi_t$ and $\overline{s}_t$:

$$\pi_t = -\frac{\overline{s}_t}{\overline{x}_t^{target} - y} - \frac{r\frac{d\overline{x}_t^{target}}{dt}}{b^2(\overline{x}_t^{target} - y)}. \tag{13}$$

The differential equation governing the dynamics of $\overline{s}_t$ is then written as follows

$$\frac{d\overline{s}_t}{dt} = -\frac{\overline{s}_t^2 b^2 + r\overline{s}_t\frac{d\overline{x}_t^{target}}{dt}}{r(\overline{x}_t^{target} - y)} + (\overline{x}_0 - y)\Big[q_{x_0} + \frac{\frac{d\overline{x}_t^{target}}{dt}}{b^2(\overline{x}_t^{target} - y)}\Big]. \tag{14}$$

To solve this differential equation numerically, we need to specify an initial condition. Since this equation is solved backwards in time, this is equivalent to determining $\overline{s}_t$. By choosing a very large $T$ control period, it is reasonable to assume that we will be very close to the steady state. We will then assimilate $q_T^y, \pi_t, \overline{s}_t$ to their steady state values when $T$ tends towards infinity, i.e. $q_\infty^y, \pi_\infty, \overline{s}_\infty$. This approximation allows us to write

$$\begin{aligned}
0 &= -\frac{b^2}{r}[\pi_\infty(\overline{x}_\infty^{target} - y) + \overline{s}_\infty], \\
0 &= \frac{b^2}{r}\pi_\infty^2 - q_\infty^y - q_{x_0}, \\
0 &= \frac{b^2}{r}\pi_\infty\overline{s}_\infty + q_{x_0}(\overline{x}_0 - y).
\end{aligned} \tag{15}$$

This yields

$$\begin{aligned} q_T^y &= q_{x_0}\Big(\frac{\overline{x}_0 - \overline{x}_\infty^{target}}{\overline{x}_\infty^{target} - y}\Big), \\ \pi_T &= \sqrt{\frac{r}{b^2}(q_{x_0} + q_T^y)}, \\ \overline{s}_T &= \pi_T(y - \overline{x}_\infty^{target}) \quad \Big(\text{or } \overline{s}_T = \frac{r q_{x_0}(y - \overline{x}_0)}{\pi_T b^2}\Big). \end{aligned} \tag{16}$$

Thereafter, we solve numerically and backwards the differential equation of $\frac{d\overline{s}_t}{dt}$, which gives us the trajectory of $\overline{s}_t$. The latter is re-injected into the equation of $\pi_t$. Finally, we have all the necessary ingredients to calculate $q_t^y$ from

$$q_t^y = \frac{b^2}{r}\pi_t^2 + \delta\pi_t - \frac{d\pi_t}{dt} - q_{x_0}. \tag{17}$$

# 3 Results in the homogeneous case

## 3.1 Data

- Homogeneous population of BEVs: we consider BEVs with $\alpha = 0.85$ and $\beta = 23\ kWh$. Note that these are *fictitious* values corresponding to average values in the more realistically formulated non homogeneous examples of the next section.
- Total daily solar energy in a parking lot: $W = 7800\ kWh$ for recharging $N = 400$ BEVs ($\overline{x}_0 = 0.15$ and $\sigma_{x_{i,0}} = 0.04$) in a typical *sunny* day, and $W = 3819\ kWh$ for recharging $N = 400$ BEVs ($\overline{x}_0 = 0.45$ and $\sigma_{x_{i,0}} = 0.1$) in a typical *cloudy* day.
- Simulation parameters: $T = 24\ h, dt = 0.01\ h$, $\nu = 0.01$, $\delta = 0.1, q_{x_0} = 1000$, $r = 0.001(kW)^{-2}$, $y = 1$ and a random distribution of $x_{i,0}$.

## 3.2 Algorithm

**Require:** $N, x_{i,0}, \overline{x}_0, \alpha, \beta, b, \delta, \nu, q_{x_0}, r, y, dt, T$ and $u_W$.
**Ensure:** Strategy $u_{i,t}^*$ for $N$ BEVs in the parking lot, $i = 1, ..., N$.

1 Solve $\frac{d\overline{x}_t^{target}}{dt} = \frac{1}{N} b u_{W_t}$ and then determine $\overline{x}_\infty^{target}$.

2 Calculate $q_T^y = q_{x_0}\Big(\frac{\overline{x}_0 - \overline{x}_\infty^{target}}{\overline{x}_\infty^{target} - y}\Big), \pi_T = \sqrt{\frac{r}{b^2}(q_{x_0} + q_T^y)}$ and $\overline{s}_T = \pi_T(y - \overline{x}_\infty^{target})$.

3 Solve $\frac{d\overline{s}_t}{dt} = -\frac{\overline{s}_t^2 b^2 + r\overline{s}_t \frac{d\overline{x}_t^{target}}{dt}}{r(\overline{x}_t^{target} - y)}$
$+(\overline{x}_0 - y)\Big[q_{x_0} + \frac{\frac{d\overline{x}_t^{target}}{dt}}{b^2(\overline{x}_t^{target} - y)}\Big]$ backwards.

4 Calculate $\pi_t = -\frac{\overline{s}_t}{\overline{x}_t^{target} - y} - \frac{r\frac{d\overline{x}_t^{target}}{dt}}{b^2(\overline{x}_t^{target} - y)}$ and determine $\frac{d\pi_t}{dt}$ (mean value theorem), $\pi_{i,t}$ (interpolation).

5 Calculate $q_t^y = \frac{b^2}{r}\pi_t^2 + \delta\pi_t - \frac{d\pi_t}{dt} - q_{x_0}$.

6 Solve $\frac{ds_{i,t}}{dt} = (\delta + \frac{b^2}{r}\pi_{i,t})s_{i,t} + q_{x_0}(x_{i,0} - y)$
backwards with $s_{i,T} = \frac{r q_{x_0}(y - x_{i,0})}{\pi_{i,T} b^2}$.

7 Calculate $u_{i,t}^* = -\frac{b}{r}\big[\pi_{i,t}(x_{i,t} - y) + s_{i,t}\big]$ with $\pi_{i,t} = \pi_t$.
knowing $dx_{i,t} = b u_{i,t} dt + \nu d\omega_i$.

## 3.3 Obtaining the average target SoC by using daily solar energy in the parking lot

Realistic generation curves based on historical meteorological data are used (Figure 1), assuming that similar generation curves can be predicted using for example, a machine learning based model. The

meteorological data is obtained from Photovoltaic Geographical Information System (PVGIS) made available by the European Commission. A typical meteorological year in the city of Montreal (45.50 North, 73.58 West) is used with a data resolution of one hour. The very same data can also be found in Canadian Weather Energy and Engineering Datasets (CWEEDS). The PV power output is then modeled with the simulation software TRNSYS using type 103 appropriate for modeling the electrical performance of mono and polycrystaline PV panels. In one isolated parking at an altitude of 64 $m$ we install 100 PV panels, each with a module area of 1.55 $m^2$, a slope of surface of 45° and an azimuth of 0°. The modules are *building-integrated*.

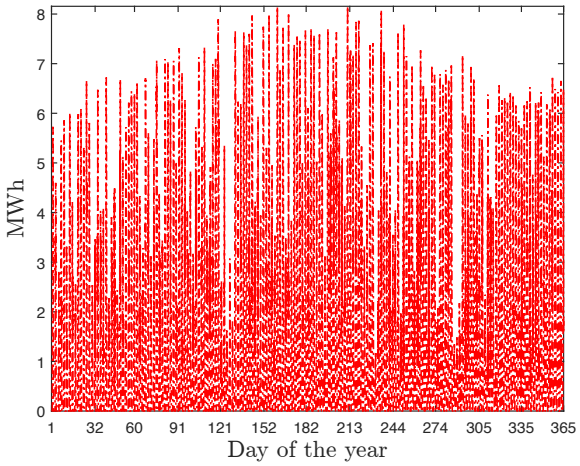


**Figure 1: Solar energy production of a 10 kW photovoltaic system with 100 panels in a parking lot in the city of Montreal (Canada) in 2015.**

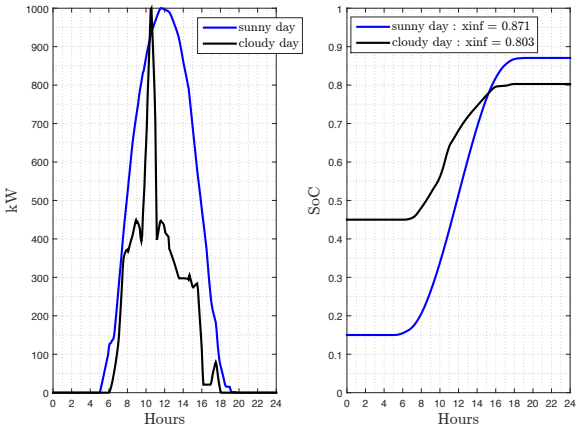


**Figure 2: Daily solar power curve $u_W$ for charging 400 homogeneous BEVs and target SoC trajectory $\overline{x}_t^{target}$ imposed by the parking lot operator.**

We determine two different real solar power curves for a full day (*sunny* day and *cloudy* day) in order to compare the influence of the difference in generation on the behaviour of the BEVs charging. Starting with a typical sunny day, and 400 homogeneous BEVs, we get an average target curve that saturates at the end of the horizon ($\overline{x}_\infty^{target} = 0.87$). Looking at a generation curve with a different profile (a cloudy day) and as a result of that a lower energy output at the end of the day, charging the same number of vehicles with the same average initial SoCs ($\overline{x}_0 = 0.15$) would result in an average target that is too low to be acceptable ($\overline{x}_\infty^{target} = 0.50$). The parking lot operator will then announce the situation the day before, so that the BEVs arrive next day more full in the parking lot. The expected

average initial SoCs is thus increased ($\overline{x}_0 = 0.45$). We get an average target curve that saturates at a more acceptable level ($\overline{x}_\infty^{target} = 0.80$). In a practical case, this latter requirement would likely result in initial SoCs with higher dispersion (*increase of standard deviation*) as some of the BEVs could meet unforeseen events.

## 3.4 Pressure field from inverse Nash, empirical per BEV average SoC and individual SoCs of BEVs using MFG

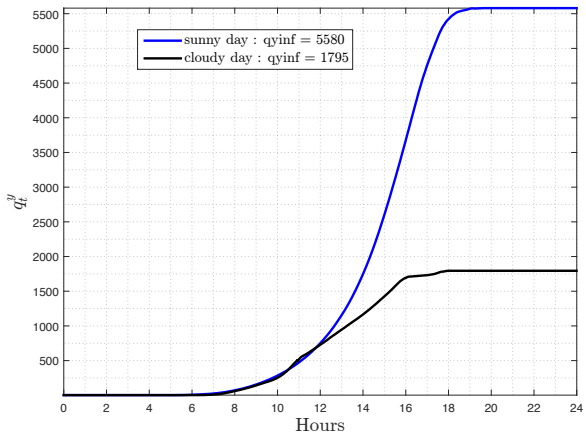


**Figure 3: Pressure field $q_t^y$ of 400 homogeneous BEVs.**

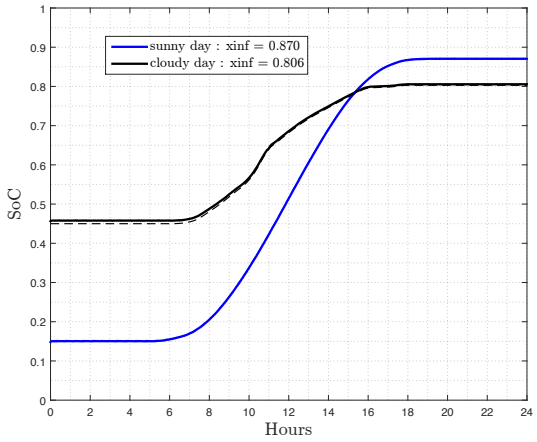


**Figure 4: Empirical per BEV average SoC $\overline{x}_t$ of 400 homogeneous BEVs.**

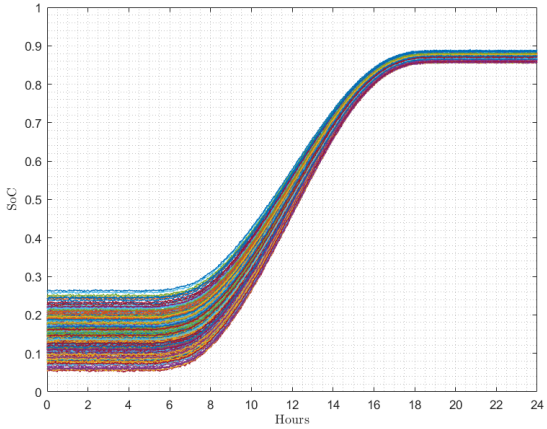


**Figure 5: Individual SoCs of 400 homogeneous BEVs in a sunny day.**

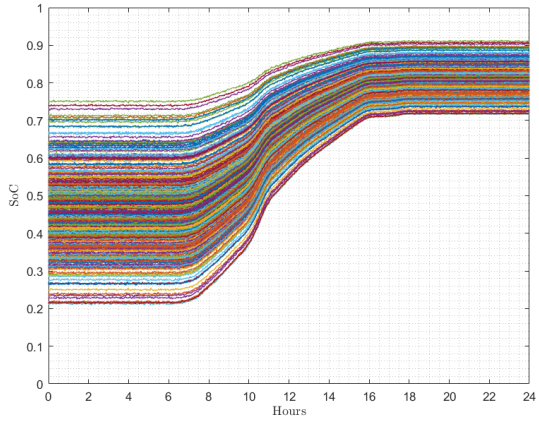


**Figure 6: Individual SoCs of 400 homogeneous BEVs in a cloudy day.**

As expected, in steady state we have a constant pressure field ($q_\infty^y$) for both days. We observe that $q_t^y$ is reduced in a typical cloudy day relative to a typical sunny day. This is because the charging rate needed to achieve full solar utilization is lower on a cloudy day. The smart charger in the parking lot needs 12 hours to fill a BEV (SoC from 0.148 to 0.870 *on average*) with a mean charging rate of 1.629 $kW$ in a typical sunny day, while it needs 11 hours in a typical cloudy day (SoC from 0.456 to 0.806 *on average*) with a mean charging rate of 0.860 $kW$. We then show that the empirical per car average SoC obtained and the target SoC imposed by the parking lot operator are quite the same, thanks to the law of large numbers. The results of individual SoCs of BEVs in both typical days show a *strong reduction in standard deviation* $\sigma_{x_{i,\infty}}$. Also, all the curves' behaviour in a typical cloudy day well reflects the characteristic of solar fluctuations. Furthermore, we confirm the main features of our

MFG control, that of *filling more batteries that were emptier to start with while bringing all batteries close to a predefined mean target.*

## 3.5 Charging controls

In the following, we present the results for the three main controls:

1. ***First come firs full*** (FCFF), which fills all the BEVs in the order of arrivals in the parking lot at maximum charging capacity. So $x_{i,\infty} = 1$ if energy available.
2. ***Equal sharing*** (ES), which fills all the BEVs in the parking lot with the same quantity. The parking lot operator calculates this quantity which depends on the quantities $\overline{x}_{\infty}^{target}$ and $\overline{x}_0$.
3. ***Mean Field Game*** (MFG), which fills all the BEVs by using the *inverse Nash algorithm.*

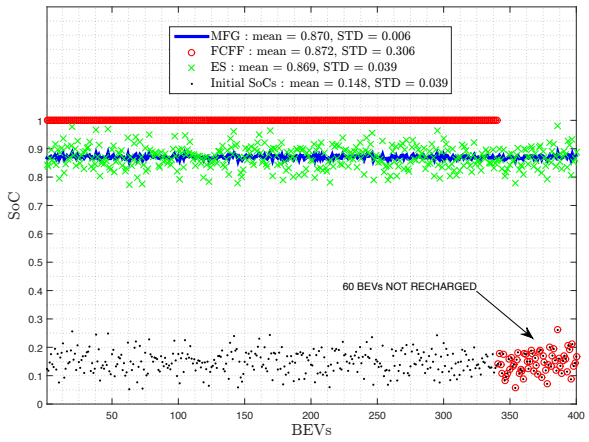


**Figure 7:** 400 **homogeneous BEVs charging controls in a sunny day.**

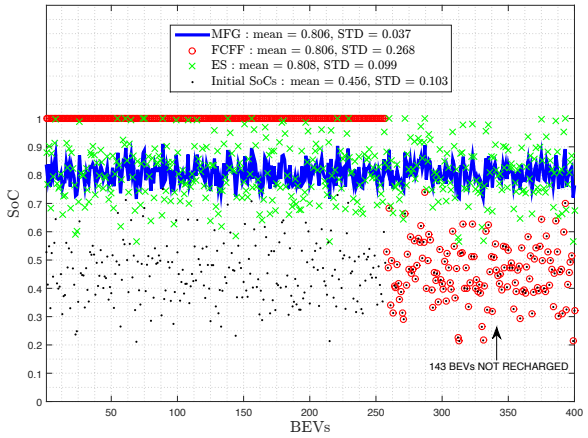


**Figure 8:** 400 **homogeneous BEVs charging controls in a cloudy day.**

## 3.6 Comparison of charging controls

### FCFF control

It is the easiest control to implement. The parking lot operator does not need to estimate an average level at the end of recharging ($\overline{x}_{\infty}^{target}$) for all BEVs. A command is sent to fulfill maximally the BEVs

in the parking lot regardless of their initial state $x_{i,0}$ only depending on their arrival times. This approach is not suitable at all for our problem. It does not meet any of the requirements. First, it is a centralized control since the parking lot operator must not only note the order of arrivals of BEVs in the parking lot, but also when they finish filling up. Secondly, at the end of the day, there will generally be users who have not recharged their batteries at all (15% of BEVs for a sunny day and 36% of BEVs for a cloudy day). So, at the end of daily recharging we will end up with very frustrated users. We have the highest values of SoCs' standard deviations: $\sigma_{x_{i,\infty}} = 0.306$ (increase of 685%) as $\overline{x}_\infty = 0.872$ for a sunny day and $\sigma_{x_{i,\infty}} = 0.268$ (increase of 160%) as $\overline{x}_\infty = 0.806$ for a cloudy day.

### ES control

This is a straightforward charging scheme. Using the forecast solar power available throughout the day, the parking lot operator estimates at all times an average level per car available for charging. As BEVs get charged, the number of cars still in demand must be updated. Thus this scheme, although superior to the previous one, is not decentralized. By giving the same amount to everyone, one does not reward individuals who took the risk to arrive at the parking lot with a lower initial SoC, so as to potentially sell more energy back to the grid during the evening peak. Lastly, the SOCs at the end of recharging ($x_{i,\infty}$) remain dispersed. Indeed, the SoCs' standard deviation remains close to what it was at the start of the day, except for a slight possible reduction due to some BEVs completely filling up.

### MFG control

This is the control we implemented in the article. The parking lot operator, after estimating $\overline{x}_\infty^{target}$, prescribes a decentralized control via our *inverse Nash algorithm* in the smart charger in the parking lot. Each user applies their optimal control locally so that, the average trajectory ($\overline{x}_t$) of all users corresponds to the average target trajectory ($\overline{x}_t^{target}$) imposed by the parking lot operator. This approach meets all the requirements of our problem. The standard deviation at the end of recharging ($\sigma_{x_{i,\infty}} = 0.006$ as $\overline{x}_\infty = 0.870$ for a sunny day and $\sigma_{x_{i,\infty}} = 0.037$ as $\overline{x}_\infty = 0.806$ for a cloudy day) has been significantly reduced (a reduction of 85% for a sunny day and 64% for a cloudy day). Although its implementation appears more complex when compared to the alternative approaches, it is a price which might be worth paying to guarantee a *robust* charging/discharging modulation system for BEVs. In turn, the latter would enhance the chances of the BEVs contributing to the expansion of the renewable energy economy.

We conclude by computing the *fairness coefficient* (FC), as illustrated in *Appendix C*, in each strategy.

**Table 2: Fairness coefficient (FC) in each charging control for** 400 **homogeneous BEVs as we know** $\min x_{i,0} = 0.05, \max x_{i,0} = 0.26$ **in a sunny day and** $\min x_{i,0} = 0.21, \max x_{i,0} = 0.75$ **in a cloudy day.**

| | *Sunny day* | | | | *Cloudy day* | | | |
|---|---|---|---|---|---|---|---|---|
| | $\min x_{i,\infty}$ | $\max x_{i,\infty}$ | $\eta$ | FC | $\min x_{i,\infty}$ | $\max x_{i,\infty}$ | $\eta$ | FC |
| *FCFF* | 0.06 | 1 | 0.12 | −0.32 | 0.21 | 1 | 0.23 | −0.27 |
| *ES* | 0.77 | 0.98 | 0 | 0 | 0.56 | 1 | 0 | 0 |
| *MFG* | 0.86 | 0.89 | 0 | 0.99 | 0.72 | 0.91 | 0 | 0.34 |

Considering the ES control as a *base case* for comparison purposes. In a typical sunny day the MFG control is 99% times fairer while FCFF is 32% less fair, and in the typical cloudy day the MFG control is 34% times fairer while FCFF is 27% less fair.

# 4 Extension: Heterogeneous population of BEVs

## 4.1 Redefinition of the problem

We consider here the case of a large heterogeneous population of BEVs. We assume that it is possible to group the BEVs into *classes considered homogeneous*. Thus, all the BEVs of a class $c$ share the same physical parameters, and have an average initial SoC $\overline{x}_{0,c}$.
Let $N$ BEVs be distributed in $C$ homogeneous classes $N_c$ such that $\sum_{c=1}^{C} N_c = N$.

Each class then possesses its own set of physical parameters $\{\alpha_c, \beta_c, b_c = \frac{\alpha_c}{\beta_c}\}$. The SoC stochastic dynamics of BEV $i$ of the $c$ class is written as follows:

$$dx_{i,t,c} = b_c u_{i,t,c} dt + \nu d\omega_i, \ t \geq 0. \tag{18}$$

The distribution of daily solar energy in each class for recharging BEVs in the parking lot, $W_c$, is calculated as follows:

$$W = \sum_{c=1}^{C} W_c, \ W_c = \sum_{t} \frac{\epsilon_c}{\sum_{i=1}^{C} \epsilon_c} u_{W_t}, \ \epsilon_c = \frac{N_c \beta_c}{\overline{x}_{0,c} \alpha_c}. \tag{19}$$

In order to better redistribute energy according to individual car needs, $W_c$ is distributed by favoring a class with more BEVs ($N_c$), a larger-size battery ($\beta_c$), a lower charging efficiency ($\alpha_c$) and finally a lower initial average ($\overline{x}_{0,c}$).

Based on this principle, the inverse Nash algorithm is used to solve the control problem *separately* for each homogeneous class of BEVs assuming that:

- the parking lot operator knows the number of total BEVs ($N$), the number of BEVs in each class ($N_c$) and the initial SoCs $x_{i,0,c}$ of the BEVs in each class.
- the parking lot operator knows the daily total solar energy ($W$) and then obtains the average target trajectories $\overline{x}_{t,c}^{target}$ of BEVs in each class. This allows her to calculate the average target trajectories $\overline{x}_{\infty,c}^{target}$ at the end of recharging in each class according to the Equations (18) and (19).
- each BEV's user knows the class she belongs to, therefore may calculate her pressure field $q_{t,c}^{y}$ and later on, her optimal control $u_{i,t,c}^{*}$ such that on average the class's trajectory ($\overline{x}_{t,c}$) corresponds to the average target trajectory of the class ($\overline{x}_{t,c}^{target}$) imposed by the parking lot operator.

## 4.2 Data

We assume that our population consists of 4 types of BEVs.

1. Class 1: $N_1$ BEVs with $\alpha = 0.8$ and $\beta = 16\ kWh$.
2. Class 2: $N_2$ BEVs with $\alpha = 0.9$ and $\beta = 16\ kWh$.
3. Class 3: $N_3$ BEVs with $\alpha = 0.8$ and $\beta = 30\ kWh$.
4. Class 4: $N_4$ BEVs with $\alpha = 0.9$ and $\beta = 30\ kWh$.

For all other parameters, we use the same values as for the homogeneous case.

## 4.3 Algorithm

The algorithm is practically the same as in the homogeneous case except that here we separate the heterogeneous BEVs into homogeneous classes to which we attribute a fraction of the total daily solar energy available.

## 4.4 Obtaining the average target SoC in each class by using daily solar energy in the parking lot

We assume the same solar generation profiles, so the total daily solar energy $W = 7800\ kWh$ for a typical *sunny day* and $W = 3819\ kWh$ for a typical *cloudy day*.

Depending on the average initial SoCs in each class ($\overline{x}_{0,c}$), our results will confirm that the daily solar energy in each class $W_c$ is well distributed by favoring the class with most BEVs and, BEVs with large battery and low charging efficiency. When $W$ is too low to satisfactorily refill all BEVs in each class, we need again to increase $\overline{x}_{0,c}$.

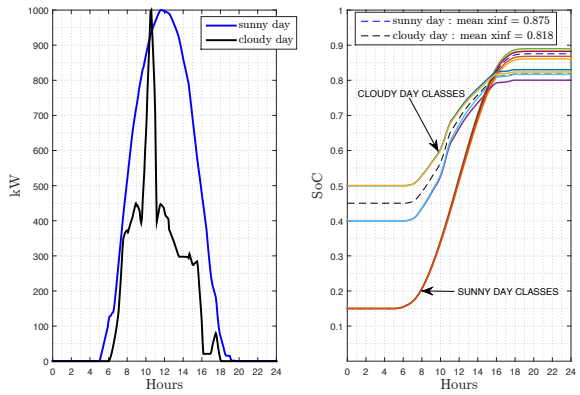


**Figure 9: Daily solar power curve $u_W$ for charging 400 heterogeneous BEVs and target SoC trajectory $\overline{x}_{t,c}^{target}$ imposed by the parking lot operator in each class.**

**Table 3: Charging 400 heterogeneous BEVs in a typical sunny day.**

| Parameters | Class 1 | Class 2 | Class 3 | Class 4 |
|---|---|---|---|---|
| $N_c$ | 98 | 102 | 101 | 99 |
| $\overline{x}_{0,c}$ | 0.15 | 0.15 | 0.15 | 0.15 |
| $\sigma_{x_{i,0,c}}$ | 0.04 | 0.04 | 0.04 | 0.04 |
| $W_c$ | 1408 $kWh$ | 1302 $kWh$ | 2720 $kWh$ | 2370 $kWh$ |
| $W$ distribution | 18.0% | 16.7% | 34.9% | 30.4% |
| $\overline{x}_{\infty,c}^{target}$ | 0.861 | 0.890 | 0.883 | 0.868 |

**Table 4: Charging 400 heterogeneous BEVs (with different high values of $\overline{x}_{0,c}$) in a typical cloudy day.**

| Parameters | Class 1 | Class 2 | Class 3 | Class 4 |
|---|---|---|---|---|
| $N_c$ | 98 | 102 | 101 | 99 |
| $\overline{x}_{0,c}$ | 0.4 | 0.4 | 0.5 | 0.5 |
| $\sigma_{x_{i,0,c}}$ | 0.1 | 0.1 | 0.1 | 0.1 |
| $W_c$ | 793 $kWh$ | 733 $kWh$ | 1225 $kWh$ | 1068 $kWh$ |
| $W$ distribution | 20.7% | 19.2% | 32.1% | 28.0% |
| $\overline{x}_{\infty,c}^{target}$ | 0.800 | 0.817 | 0.830 | 0.824 |

NOTE : Since we have less daily solar energy ($W = 3819\ kWh$), we will require users with a *large battery* to come a little fuller than others.

## 4.5 Pressure field in each class from inverse Nash, empirical per BEV average SoC in each class and individual SoCs of BEVs using MFG

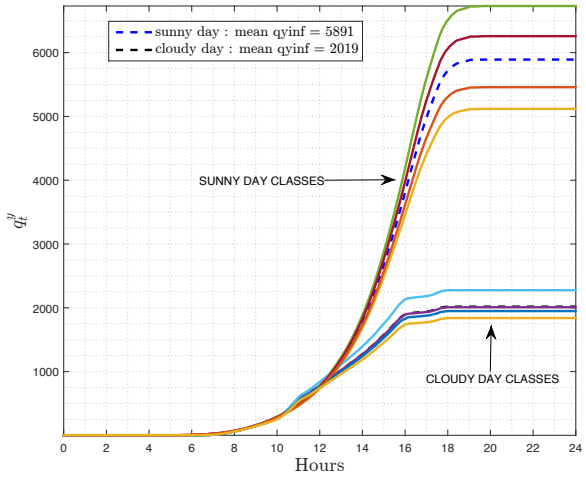


**Figure 10: Pressure fields $q^y_{t,c}$ of 400 heterogeneous BEVs.**

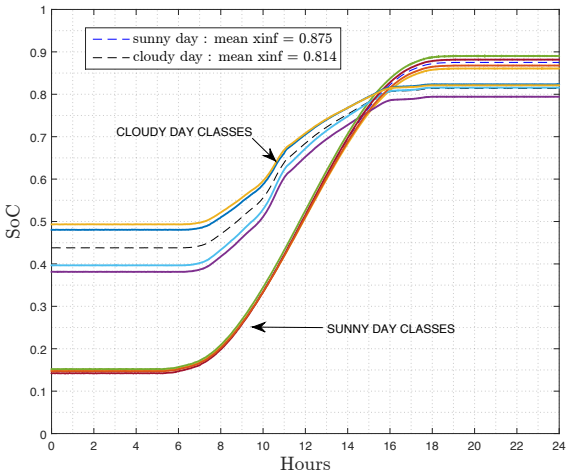


**Figure 11: Empirical per BEV average SoCs $\overline{x}_{t,c}$ of 400 heterogeneous BEVs.**

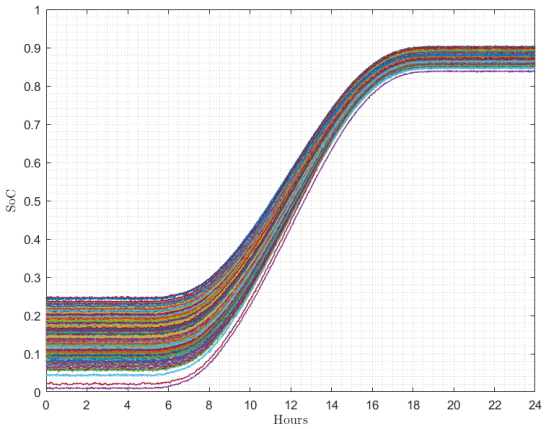


**Figure 12: Individual SoCs of 400 heterogeneous BEVs in a sunny day.**

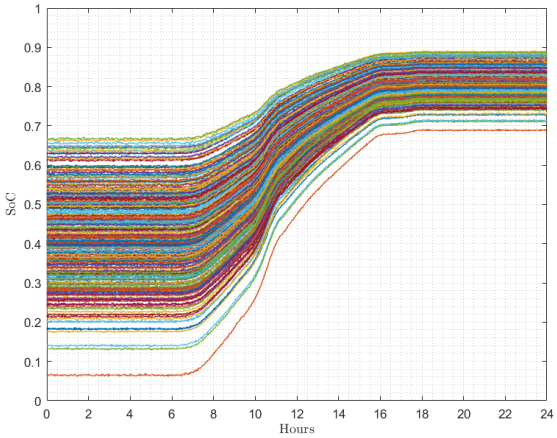


**Figure 13: Individual SoCs of 400 heterogeneous BEVs in a cloudy day.**

As expected, in steady state we have constant pressure fields ($q^y_{\infty,c}$) in each class for both days. The pressure $q^y_{\infty,c}$ increases with the difference $(\overline{x}^{target}_{\infty,c} - \overline{x}_{0,c})$ for both days. The smart charger in the parking lot needs 12 hours to fill a BEV (SoC from 0.147 to 0.875 *on average*) with a mean charging rate of 1.642 $kW$ on a typical sunny day, while it needs 11 hours on a typical cloudy day (SoC from 0.434 to 0.814 *on average*) with a mean charging rate of 0.935 $kW$. Then, we show that the empirical per car average SoC obtained and the target SoC imposed by the parking lot operator are quite close, thanks to the law of large numbers. The results of individual SoCs of BEVs in both days also demonstrate a *reduction in standard deviation* but *less* than what we had in the homogeneous case. Finally, the behaviour of all curves in a typical cloudy day closely reflects the characteristics of solar fluctuations.

## 4.6 Charging controls

The charging controls, as defined previously, fill all the BEVs *in regard to their class* in the heterogeneous case.

**Table 5: Charging controls in each class for 400 heterogeneous BEVs in a typical sunny day.**

| | Class 1 | | Class 2 | | Class 3 | | Class 4 | |
|---|---|---|---|---|---|---|---|---|
| | $\overline{x}_{\infty,1}$ | $\sigma_{x_{i,\infty,1}}$ | $\overline{x}_{\infty,2}$ | $\sigma_{x_{i,\infty,2}}$ | $\overline{x}_{\infty,3}$ | $\sigma_{x_{i,\infty,3}}$ | $\overline{x}_{\infty,4}$ | $\sigma_{x_{i,\infty,4}}$ |
| *FCFF* | 0.867 | 0.315 | 0.893 | 0.282 | 0.883 | 0.293 | 0.869 | 0.312 |
| *ES* | 0.860 | 0.041 | 0.892 | 0.041 | 0.875 | 0.040 | 0.865 | 0.041 |
| *MFG* | 0.861 | 0.006 | 0.890 | 0.005 | 0.882 | 0.005 | 0.868 | 0.006 |
| $\overline{x}_{0,c}, \sigma_{x_{i,0,c}}$ | 0.149 | 0.041 | 0.152 | 0.041 | 0.142 | 0.040 | 0.147 | 0.041 |

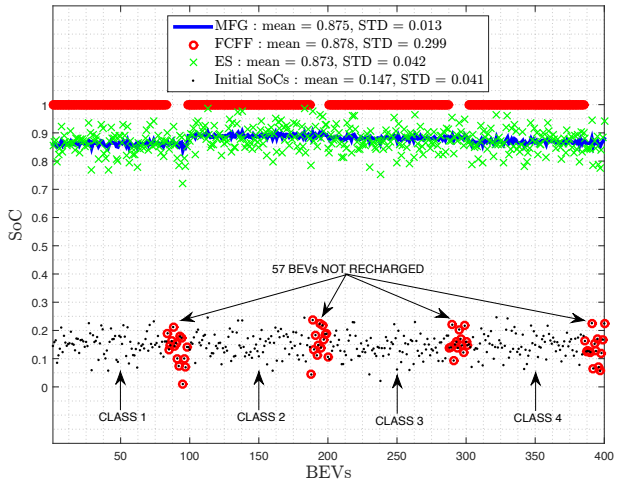


**Figure 14: 400 heterogeneous BEVs charging controls in a sunny day.**

Considering a typical *sunny day*, the MFG control is clearly the best between the three options insofar as the *resulting standard deviation* for all classes at the end of recharging is concerned ($\overline{\sigma}_{x_{i,\infty}} = 0.013$, reduction of 68% with $\overline{x}_{\infty} = 0.875$). With the FCFF control we still have frustrated users who have not recharged their batteries at all (14% of BEVs) with the worst standard deviation at the end of recharging ($\overline{\sigma}_{x_{i,\infty}} = 0.299$, increase of 629% with $\overline{x}_{\infty} = 0.878$). Finally, with the ES control, we have a very small increase of 2% of the standard deviation at the end of recharging ($\overline{\sigma}_{x_{i,\infty}} = 0.042$ with $\overline{x}_{\infty} = 0.873$) due to more dispersed initial SoCs $x_{i,0,c}$, as it was not the case for the homogeneous BEVs. The SoCs at the end of recharging are little more dispersed and that may compromise the BEVs' willingness to return energy in the evening peak to the grid.

**Table 6: Charging controls in each class for 400 heterogeneous BEVs in a typical cloudy day.**

| | Class 1 | | Class 2 | | Class 3 | | Class 4 | |
|---|---|---|---|---|---|---|---|---|
| | $\overline{x}_{\infty,1}$ | $\sigma_{x_{i,\infty,1}}$ | $\overline{x}_{\infty,2}$ | $\sigma_{x_{i,\infty,2}}$ | $\overline{x}_{\infty,3}$ | $\sigma_{x_{i,\infty,3}}$ | $\overline{x}_{\infty,4}$ | $\sigma_{x_{i,\infty,4}}$ |
| *FCFF* | 0.800 | 0.303 | 0.821 | 0.284 | 0.824 | 0.247 | 0.823 | 0.258 |
| *ES* | 0.782 | 0.105 | 0.812 | 0.097 | 0.811 | 0.102 | 0.816 | 0.090 |
| *MFG* | 0.794 | 0.035 | 0.816 | 0.031 | 0.824 | 0.034 | 0.821 | 0.032 |
| $\overline{x}_{0,c}, \sigma_{x_{i,0,c}}$ | 0.381 | 0.106 | 0.397 | 0.101 | 0.480 | 0.102 | 0.493 | 0.091 |

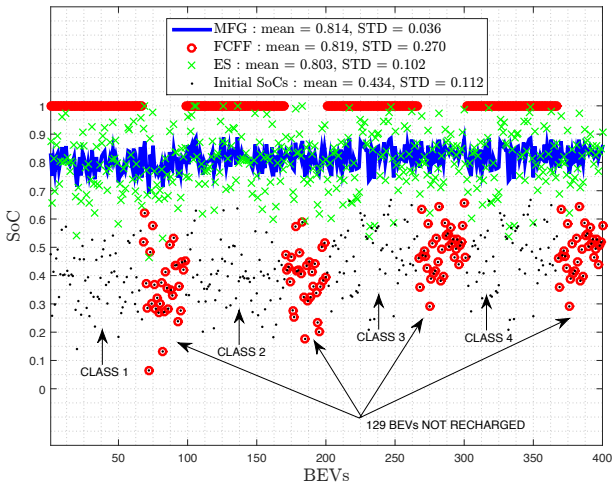


**Figure 15:** 400 **heterogeneous BEVs charging controls in a cloudy day.**

Considering a typical *cloudy day*, the MFG control remains the best between the three options from the point of view of *resulting standard deviation* for all classes at the end of recharging ($\overline{\sigma}_{x_{i,\infty}} = 0.036$, reduction of 68% with $\overline{x}_{\infty} = 0.814$). With the FCFF control we have here a significant fraction of frustrated users who have not recharged their batteries at all (32% of BEVs) with, once again, the worst standard deviation at the end of recharging ($\overline{\sigma}_{x_{i,\infty}} = 0.270$, increase of 141% with $\overline{x}_{\infty} = 0.819$). Finally, with the ES control, we have at the end of recharging a slightly reduced standard deviation ($\overline{\sigma}_{x_{i,\infty}} = 0.102$, reduction of 9% with $\overline{x}_{\infty} = 0.803$) relative to that at the start of recharging ($\overline{\sigma}_{x_{i,\infty}} = 0.112$) as a few BEVs exceed their maximum level.

We conclude by computing the *fairness coefficient* (FC), as illustrated in *Appendix C*, for each strategy.

**Table 7: Fairness coefficient (FC) in each charging control for** 400 **heterogeneous BEVs as we know** $\min x_{i,0} = 0.01, \max x_{i,0} = 0.25$ **in a sunny day and** $\min x_{i,0} = 0.06, \max x_{i,0} = 0.67$ **in a cloudy day.**

| | *Sunny day* | | | | *Cloudy day* | | | |
|---|---|---|---|---|---|---|---|---|
| | $\min x_{i,\infty}$ | $\max x_{i,\infty}$ | $\eta$ | FC | $\min x_{i,\infty}$ | $\max x_{i,\infty}$ | $\eta$ | FC |
| *FCFF* | 0.01 | 1 | 0.12 | −0.30 | 0.06 | 1 | 0.23 | −0.21 |
| *ES* | 0.72 | 0.98 | 0 | 0 | 0.46 | 1 | 0 | 0 |
| *MFG* | 0.84 | 0.90 | 0 | 0.42 | 0.69 | 0.89 | 0 | 0.38 |

Considering the ES control as a *base case* for comparison purposes. In a typical sunny day the MFG control is 42% times fairer while FCFF is 30% less fair, and in the typical cloudy day the MFG control is 38% times fairer while FCFF is 21% less fair.

# 5 Conclusion and future research

We have considered the situation of a large daytime work parking lot exclusively for battery electric vehicles (BEVs), with solar sources based electricity charging. We have used realistic data to implement deterministic daily solar power curves with photovoltaic panels in a parking lot for a typical sunny day and a typical cloudy day. A *fair* and *decentralized* MFG control for recharging BEVs has been developed considering, first in the case of a large fixed homogeneous population, and subsequently that of a heterogeneous population. *The goal was to reduce significantly the SoCs' standard deviation while maintaining everyone at a high satisfactorily level regardless of their SoCs' initial states.* A comparison was carried out with a *first come first full* control and an *equal sharing* control which we saw could

result in some unsatisfied individual users with little SoCs at the end of recharging. Also, we did much better than the literature [10, 19] as we illustrated in the summary Tables 8 and 9 when we compared our results to the base case which is here the *equal sharing* control. The minimum standard deviation is 60% while we have dealt with *all possible cases*.

**Table 8: Standard deviation increase/reduction for homogeneous and heterogeneous BEVs in a large-size parking lot.**

| | 400 *homogeneous* BEVs in a sunny day | in a cloudy day | 400 *heterogeneous* BEVs in a sunny day | in a cloudy day |
|---|---|---|---|---|
| *FCFF* | $\uparrow 685\%$ | $\uparrow 171\%$ | $\uparrow 612\%$ | $\uparrow 165\%$ |
| *MFG* | $\downarrow 85\%$ | $\downarrow 63\%$ | $\downarrow 69\%$ | $\downarrow 65\%$ |
| $\sigma_{x_{i,0}}$ | 0.04 | 0.1 | 0.04 | 0.1 |
| $\overline{x}_0 \to \overline{x}_\infty$ | $0.148 \to\approx 0.870$ | $0.456 \to\approx 0.806$ | $0.147 \to\approx 0.875$ | $0.434 \to\approx 0.810$ |

In *appendix B*, we show that our MFG control remains the best way to share daily solar energy in a small-size parking lot with very few BEVs. Indeed, because of the *linearity* of SOC's model, the analysis is perfectly exact for arbitrarily small numbers of cars if the battery charging processes are deterministic.

**Table 9: Standard deviation increase/reduction for homogeneous BEVs in a small-size parking lot.**

| | 50 *homogeneous* BEVs $\sigma_{x_{i,0}} = 0.1 \to \sigma_{x_{i,\infty}}$ | in a sunny day $\overline{x}_0 \to \overline{x}_\infty$ | 10 *homogeneous* BEVs $\sigma_{x_{i,0}} = 0.2 \to \sigma_{x_{i,\infty}}$ | in a cloudy day $\overline{x}_0 \to \overline{x}_\infty$ |
|---|---|---|---|---|
| *FCFF* | $\uparrow 160\%$ | $0.154 \to 0.938$ | $\uparrow 38\%$ | $0.467 \to 0.799$ |
| *MFG* | $\downarrow 89\%$ | $0.154 \to 0.930$ | $\downarrow 60\%$ | $0.467 \to 0.789$ |

In future work, we wish to extend our work by considering a fluctuating population of BEVs and all aggregate targets will be set by considering day ahead forecasts of traffic patterns (this will result in an agent optimization problem following a machine learning process [17]), solar energy availability and evening power system load updated with the latest information when useful. The very same Mean Field Games analysis will then be carried in the grid for BEVs returning to their residences.

## Credit authorship contribution statement

**Samuel M. Muhindo** : Conceptualization, Methodology, Writing - Original Draft, Related Work, Validation, Software, Writing - Review & Editing.

**Roland P. Malhamé** : Conceptualization, Methodology, Writing - Review & Editing, Supervision, Funding acquisition.

**Géza Joós** : Conceptualization, Writing - Review & Editing, Funding acquisition.

## Declaration of competing interest

The authors declare that they have no known competing financial interests or personal relationships that could have appeared to influence the work reported in this paper.

# Appendix

## A Mean Field Game theory

### Basic concepts – Game theory

Given a set of $N$ agents in a classic game, each agent is looking to maximize its happiness. The latter is assimilated to a cost function that the agent wants to minimize. This one depends on the strategy $u_{i,t}$ of the agent $i$, of its state $x_{i,t}$, but also of the strategies of all the others, noted $u_{-i,t}$. Such a function can be written as follows:

$$J_i(u_{i,t}) = \sum_{j=1}^{N} L(x_{i,t}, u_{i,t}, x_{j,t}). \tag{20}$$

The solution concept for such a game consists in finding a *Nash equilibrium*, i.e. a set of strategies $(u_{i,t})^*$, such that any deviation of an agent $i$ from its strategy $(u_{i,t})^*$, knowing that the other agents apply $(u_{-i,t})^*$, is damaging to her (her cost is increasing). This involves calculating all the interactions between each pairs of agents, which is extremely costly if the number of agents is large.

### Principle of Mean Field Games

Mean Field Games (MFG) are a theoretical framework for dealing with problems of non-cooperative games in which a large number of agents participate. However, an important specificity of these games is that the impact of individual agents becomes asymptotically negligible as the numbers grow without bound. Instead of the individual interactions between each agent, it is then the collective dynamics of all the agents (as represented by the flow of their empirical state distribution) that is considered in the calculation of the optimal strategy of the individuals [8]. This approximation greatly simplifies the calculations and makes it possible to consider the modelling of a large number of agents while maintaining a moderate calculation time. The shift from a pair-to-pair interaction computation to a generic agent interaction with the distribution of the whole set of agents is the cornerstone of the simplification brought about by MFG. MFG related ideas can already be found in the works of Jovanovic and Rosenthal in the Economics community in 1988. But MFG actual formalization is due to the pioneering work in 2006 of Lasry and Lions in the Mathematics community and, Huang, Caines and Malhamé in the Engineering community [2, 8].

### Mathematical Formulation of Mean Field Games

We consider a set of $N$ agents whose actions take place over a finite time horizon $T$. Their state is noted $x_{i,t} \in \mathbb{R}^n, 1 \leq i \leq N$. By noting $u_{i,t} \in \mathbb{R}^m$ the strategy of the agent $i$, we can define the dynamics of this agent as

$$dx_{i,t} = \frac{1}{N} \sum_{j=1}^{N} f(x_{i,t}, u_{i,t}, x_{j,t})dt + \nu d\omega_i, \tag{21}$$

where $\omega_i$ is a Brownian process, assuming independent processes between each agent, and $\nu$ the Brownian noise. Note that other noise models are also possible.

For a finite horizon, the cost function is written as the mean of the integral of the pairwise interaction costs with each of the other agents:

$$J_i(x_{i,0}, u_{i,t}) = \mathbb{E}\Big[ \int_0^T \frac{1}{N} \sum_{j=1}^{N} L(x_{i,t}, u_{i,t}, x_{j,t})dt \mid x_{i,0} \Big]. \tag{22}$$

It should be noted that the extension to an infinite horizon is possible by adding the exponential $e^{-\delta t}$ to ensure convergence of the cost, where $\delta$ is a discount factor.

### Linear Quadratic Gaussian (LQG) Mean Field Games

We consider, for simplicity, the scalar case of homogeneous agents with linear dynamics

$$dx_{i,t} = (ax_{i,t} + bu_{i,t})dt + \nu d\omega_i, \tag{23}$$

and the $i$ cost function associated is

$$J_i(x_{i,0}, u_{i,t}) = \mathbb{E}\Big[\int_0^\infty e^{-\delta t}\big[q(x_{i,t} - \Phi(\overline{x}^{(N)}))^2 + ru_{i,t}^2\big]dt \mid x_{i,0}\Big], \tag{24}$$

with $\Phi(\cdot)$ and $q(\cdot)$ could be arbitrary nonlinear functions. Note that this cost function was initially inspired by cellular telephone power control applications [8].

Here, the $\overline{x}^{(N)} := \frac{1}{N}\sum_{j=1}^{N} x_j$ is the mean field influence term as the number of agents $N$ goes to infinity. Asymptotically, it becomes the *deterministic* (yet so far unknown) mean state trajectory of the agents denoted $\overline{x}(t)$. At that stage, the agent knows that because its influence on the mean field vanishes, it can consider the $\bar{x}(t)$ as a decoupled *frozen* trajectory. Thus, interestingly, as $N \to \infty$, a generic agent needs only to solve a standard discounted optimal linear quadratic tracking problem instead of a full fledged infinite population game, with possible push-back from other agents.

Solving this game requires formulating and solving a *backwards Hamilton-Jacobi-Bellman* equation according to the principle of dynamic programming [1]. This resolution comes down to that of a set of Riccati equations [8, 9] thus providing the optimal strategy for the agent $i$. This solution is re-injected into $dx_{i,t}$ to give the optimal evolution of the agent.

## B Mean Field Game-based control of sharing daily solar energy between BEVs in a small-size parking lot

We will illustrate that even with very few BEVs in a small-size parking lot, our MFG control will remain the best way to share daily solar energy due to the *linearity* of the BEV's SoC model. We only study here the case of *homogeneous* BEVs (battery parameters $\alpha = 0.8$ and $\beta = 16\ kWh$).

First, we consider a parking lot with 10 PV panels (total daily solar energy $W = 780\ kWh$) that can accommodate up to 50 BEVs in a typical *sunny day*. Then, we consider a parking lot with 2 PV panels (total daily solar energy $W = 66\ kWh$) that can accommodate up to 10 BEVs in a typical *cloudy day*. These are the results:

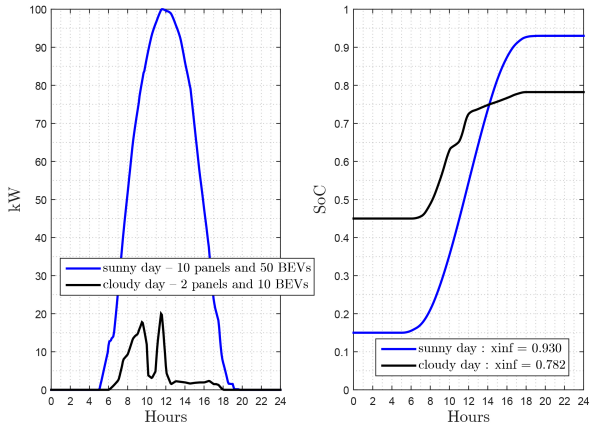


**Figure 16: Daily solar power curve $u_W$ for charging homogeneous BEVs and target SoC trajectory $\overline{x}_t^{target}$ imposed by the parking lot operator.**

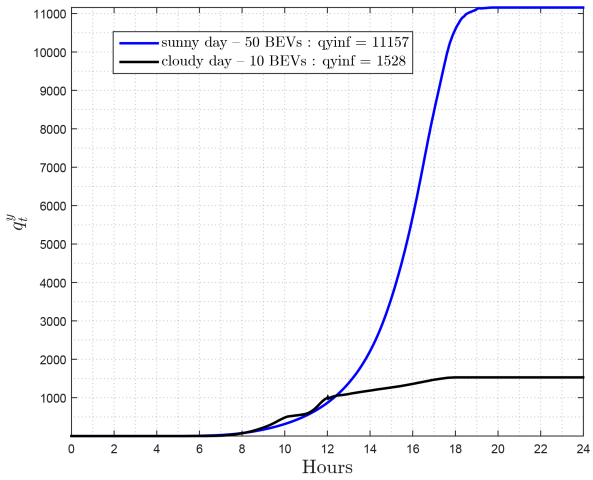


**Figure 17: $q_t^y$ resulting from inverse Nash calculation.**

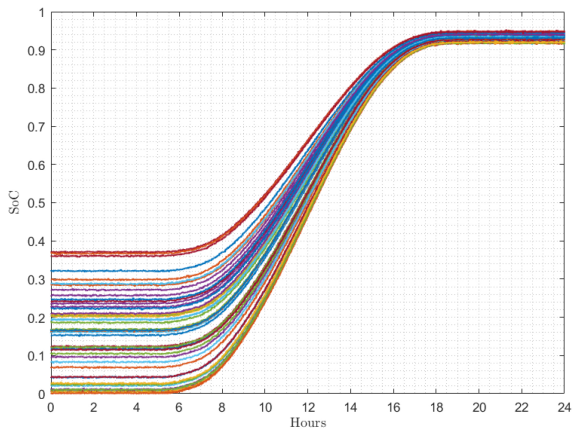


**Figure 18: Individual SoCs of $50$ homogeneous BEVs in a sunny day.**

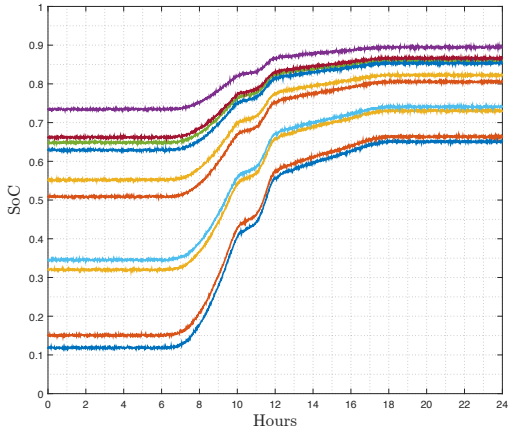


**Figure 19: Individual SoCs of $10$ homogeneous BEVs in a cloudy day.**

**Table 10: Fairness coefficient (FC) in each charging control for homogeneous BEVs as we know $\min x_{i,0} = 0, \max x_{i,0} = 0.37$ in a sunny day and $\min x_{i,0} = 0.12, \max x_{i,0} = 0.73$ in a cloudy day.**

| | *Sunny day* (50 BEVs) | | | | *Cloudy day* (10 BEVs) | | | |
|---|---|---|---|---|---|---|---|---|
| | $\min x_{i,\infty}$ | $\max x_{i,\infty}$ | $\eta$ | FC | $\min x_{i,\infty}$ | $\max x_{i,\infty}$ | $\eta$ | FC |
| *FCFF* | 0.16 | 1 | 0.10 | −0.14 | 0.15 | 1 | 0.31 | −0.12 |
| *ES* | 0.78 | 1 | 0 | 0 | 0.45 | 1 | 0 | 0 |
| *MFG* | 0.92 | 0.95 | 0 | 3 | 0.65 | 0.90 | 0 | 0.55 |

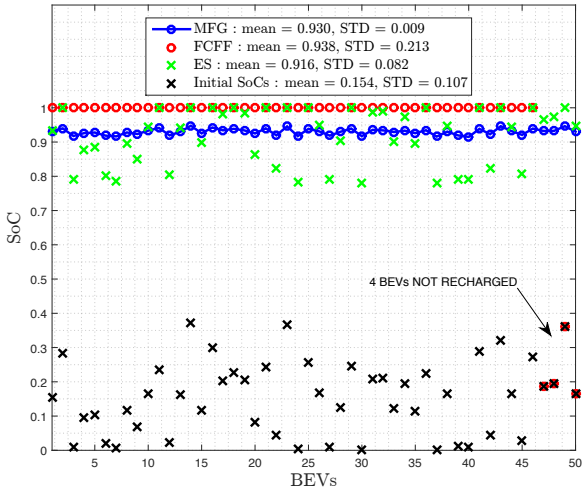


**Figure 20:** 50 **homogeneous BEVs charging controls in a sunny day.**

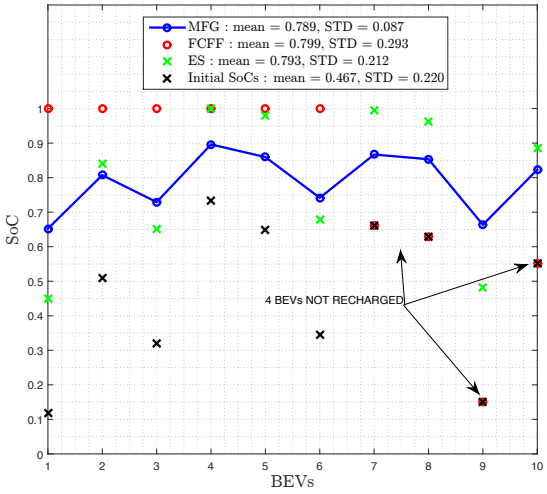


**Figure 21:** 10 **homogeneous BEVs charging controls in a cloudy day.**

# C Fairness coefficient

We evaluate the quality of a charging control according to a *fairness coefficient* (FC) which should be :

- *proportional* to a weight $\eta$ which depends on the number $N_O$ of occurrences when we have an emptier BEV at the beginning exceeds a fuller one at the end of recharging in the population of $N$ BEVs.
- *proportional* to the difference between the initial and final standard deviations of SoCs.
- *inversely proportional* to the difference between the maximum and the minimum final SoCs.

We come up with this formula:

$$FC = \frac{\sigma_{x_{i,0}} - \sigma_{x_{i,\infty}}}{\max x_{i,\infty} - \min x_{i,\infty}} \; e^{-\eta \times \mathtt{sgn}(\sigma_{x_{i,0}} - \sigma_{x_{i,\infty}})}, \tag{25}$$

where

$$\eta = \frac{N_O}{\binom{N}{2}} = \frac{2\ N_O\ (N-2)!}{N!}. \tag{26}$$

- The control is $FC\%$ *times fairer* if $FC > 0$.
- The control is *neutral* if $FC = 0$.
- The control is $FC\%$ *times less fair* if $FC < 0$.

# References

[1] Richard E. Bellman and Stuart E. Dreyfus. Applied dynamic programming. Princeton University Press, second edition edition, 12 2015.

[2] Pierre Cardaliaguet. Lecture Notes: Mean Field Games (Available online). Université Paris-Dauphine, 2013.

[3] G.R. Chandra Mouli, P. Bauer, and M. Zeman. System design for a solar powered electric vehicle charging station for workplaces. Applied Energy, 168, 4 2016. doi: 10.1016/j.apenergy.2016.01.110.

[4] Paul Denholm, Matthew O'Connell, Gregory Brinkman, and Jennie Jorgenson. Overgeneration from Solar Energy in California: A Field Guide to the Duck Chart. Technical report, National Renewable Energy Laboratory, 11 2015.

[5] Swaraj Sanjay Deshmukh and Joshua M. Pearce. Electric vehicle charging potential from retail parking lot solar photovoltaic awnings. Renewable Energy, 169, 5 2021. doi: 10.1016/j.renene.2021.01.068.

[6] Lukas Drude, Luiz Carlos Pereira Junior, and Ricardo Rüther. Photovoltaics (PV) and electric vehicle-to-grid (V2G) strategies for peak demand reduction in urban regions in Brazil in a smart grid environment. Renewable Energy, 68, 8 2014. doi: 10.1016/j.renene.2014.01.049.

[7] Raquel Figueiredo, Pedro Nunes, and Miguel C. Brito. The feasibility of solar parking lots for electric vehicles. Energy, 140, 12 2017. doi: 10.1016/j.energy.2017.09.024.

[8] Minyi Huang, Peter E. Caines, and Roland P. Malhamé. Large-Population Cost-Coupled LQG Problems With Nonuniform Agents: Individual-Mass Behavior and Decentralized $\varepsilon$-Nash Equilibria. IEEE Transactions on Automatic Control, 52(9), 9 2007. doi: 10.1109/TAC.2007.904450.

[9] Arman C. Kizilkale, Rabih Salhab, and Roland P. Malhamé. An integral control formulation of mean field game based large scale coordination of loads in smart grids. Automatica, 100, 2 2019. doi: 10.1016/j.automatica.2018.11.029.

[10] Stephen Lee, Srinivasan Iyengar, David Irwin, and Prashant Shenoy. Shared solar-powered EV charging stations: Feasibility and benefits. In 2016 Seventh International Green and Sustainable Computing Conference (IGSC). IEEE, 2016. doi: 10.1109/IGCC.2016.7892600.

[11] Quentin Lenet. Master's thesis: Contrôle décentralisé d'un ensemble de dispositifs de chauffage électrique. Polytechnique Montreal, 4 2020.

[12] Zhongjing Ma, Duncan S. Callaway, and Ian A. Hiskens. Decentralized charging control of large populations of plug-in electric vehicles. IEEE Transactions on Control Systems Technology, 21(1), 2013. doi: 10.1109/TCST.2011.2174059.

[13] Pol Olivella-Rosell, Roberto Villafafila-Robles, and Andreas Sumper. Impact evaluation of plug-in electric vehicle on power systems. In Sumedha Rajakaruna, Farhad Shahnia, and Arindam Gosh, editors, Plug in electric vehicles in smart grids: Integration Techniques, chapter 6, pages 149–178. Springer, 2015.

[14] Ricardo Rüther, Luiz Carlos Pereira Junior, Alice Helena Bittencourt, Lukas Drude, and Isis Portolan dos Santos. Strategies for plug-in electric vehicles to grid (V2G) and photovoltaics (PV) for peak demand reduction in urban regions in a smart grid environment. In Sumedha Rajakaruna, Farhad Shahnia, and Arindam Gosh, editors, Plug in electric vehicles in smart grids: Integration Techniques, chapter 7, pages 179–219. Springer, 2015. doi: 10.1007/978-981-287-299-9_7.

[15] Eric Sortomme, Mohammad M. Hindi, S. D. James MacPherson, and S. S. Venkata. Coordinated Charging of Plug-In Hybrid Electric Vehicles to Minimize Distribution System Losses. IEEE Transactions on Smart Grid, 2(1), 3 2011. doi: 10.1109/TSG.2010.2090913.

[16] Wencong Su, Jianhui Wang, and Zechun Hu. Planning, Control, and Management Strategies for Parking Lots for PEVs. In Sumedha Rajakaruna, Farhad Shahnia, and Arindam Gosh, editors, Plug in electric vehicles in smart grids: Integration Techniques, chapter 3, pages 61–98. Springer, 2015. doi: 10.1007/978-981-287-299-9_3.

[17] Felix Tuchnitz, Niklas Ebell, Jonas Schlund, and Marco Pruckner. Development and Evaluation of a Smart Charging Strategy for an Electric Vehicle Fleet Based on Reinforcement Learning. Applied Energy, 285, 3 2021. doi: 10.1016/j.apenergy.2020.116382.

[18] Erotokritos Xydas, Charalampos Marmaras, and Liana M. Cipcigan. A multi-agent based scheduling algorithm for adaptive electric vehicles charging. Applied Energy, 177, 9 2016. doi: 10.1016/j.apenergy.2016.05.034.

[19] Yingjie Zhou, Nicholas Maxemchuk, Xiangying Qian, and Yasser Mohammed. A weighted fair queuing algorithm for charging electric vehicles on a smart grid. In 2013 IEEE Online Conference on Green Communications (OnlineGreenComm). IEEE, 10 2013. doi: 10.1109/OnlineGreenCom.2013.6731041.